# Modeling Immune Search Through the Lymphatic Network

Jannatul Ferdous<sup>\*,1</sup>, G. Matthew Fricke<sup>1,2</sup>, and Melanie E. Moses<sup>1,3,4</sup>

- Department of Computer Science, University of New Mexico Albuquerque, USA
  Center for Advanced Research Computing
  Biology Department University of New Mexico, Albuquerque, USA
  - <sup>3</sup> Biology Department, University of New Mexico, Albuquerque, USA
    <sup>4</sup> Santa Fe Institute, Santa Fe, USA
    \*Corresponding Author: jannat@unm.edu

Abstract. The lymphatic system is a networked structure used by billions of immune cells, including T cells and Dendritic cells, to locate and identify invading pathogens. Dendritic cells carry pieces of pathogens to the nearest lymph node, and T cells travel through the lymphatic vessels and search within lymph nodes to find them. Here we investigate how the topology of the lymphatic network affects the time for this search to be completed. Building on prior work that maps out the human lymphatic network, we develop and extend a method to infer the lymphatic network topology of mice. We compare search times for the modeled and observed topologies and show that they are similar to each other and consistent with observed immune response times. This is relevant for translating immune response times in mice, where most experimental work occurs, into expected immune response times in humans. Our analysis predicts that for large systemic infections, the topology of the lymphatic network allows immune response times to remain fast even as animal mass increases by orders of magnitude. This work advances our understanding of how the structure of the lymphatic network supports the swarm intelligence of the immune system. It also elucidates general principles relating swarm size and organization to search speed.

# 1 Introduction

Adaptive immunity evolved in vertebrates to recognize and remember novel pathogens, enabling a faster response time to subsequent infections. In contrast to most biological rates, which are systematically slower in larger animals (scaling as  $M^{1/4}$ , where M is body mass [11, 26, 2]), the adaptive immune response time is relatively invariant across several orders of magnitude of mammalian body mass [6, 4]. Immune response is a swarm intelligence problem with billions of interacting agents searching for pathogens without central control, and it is a model for scale-invariant search in swarms.

T cells are adaptive immune cells that can recognize novel pathogens in lymph nodes, and then replicate and disperse into tissues to find and kill cells infected by those pathogens. The movement of T cells through the lymphatic system increases contact with antigens and amplifies the immune response [23]. Similar to eusocial insects, information transmission in this liquid brain [21] is mediated through direct agent contact and chemical signals among agents that navigate complex and varied environments [16].

Each T cell can bind to a particular subset of cognate antigens. Dendritic cells (DCs) gather antigen from tissues, travel to and enter nearby lymph nodes (LNs) through the lymphatic network, and display the antigen on their surfaces. T cells search LNs for DCs displaying cognate antigen, and if a match is made, the T cells activate, proliferate, and circulate to the site of infection where they kill infected cells. The time it takes to initiate an adaptive immune response depends on two factors: 1) the speed with which T cells travel through the lymphatic system to LNs containing DCs displaying antigen, and 2) how quickly T cells find those DCs once inside the LN.

In this work, we analyze T cell travel time through the lymphatic network to find DC's in mice and humans by extending the algorithm of Savinkov et al. [20], that models only the human lymphatic networks. While most lab studies that show how the immune system works are conducted on mice, most of the literature on modeling the lymphatic network is based on humans. The lack of data makes it challenging to build a general model of lymphatic networks for mice and other mammals. The model parameters are updated based on best-fit values by comparing empirically observed anatomical data with the graph resulting from the algorithm. We expand the network metrics used by the algorithm to better fit the model to empirical data. Using the inferred network model we compute the expected time for T cells to find LNs containing DCs presenting cognate antigen. We run a random walk search on the simulated and observed lymphatic networks to find the average time T cells need to reach the LNs containing cognate DCs. We find that the generated and actual anatomical graphs have similar statistics. The resulting search time over the network is similar in mice and humans for systematic or mass-dependent infections, but it is longer in humans than in mice for small infections that only reach a single LN.

# 2 Related Work

Several studies have modeled the human lymphatic system [19, 24, 20]. In [24], the authors use computational geometry to build graph models of the human lymphatic network in order to explain the general features underlying the 3D structural organization of the lymphatic system. The model is based on available anatomical data (from the PlasticBoy project [1]), which estimates the lymphatic system's structure and analyzes the topological properties of the resulting models. In [20], the authors developed and implemented a computational algorithm to generate the algorithm-based random graph of the human lymphatic system. Some fundamental characteristics of the observed data-based graph [24] and the algorithm-based graph of human lymphatic system graph models are analyzed.

In [27] Wiegel and Perelson hypothesize that LN number and size evolved to minimize two competing goals: the time to transport antigen from an infected

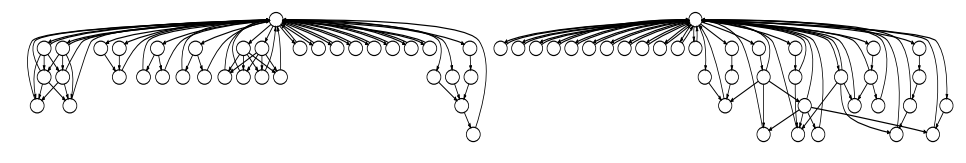


Fig. 1. Fig. 2.

**Fig. 3.** Comparison of simulated and observed lympathic networks. (a) Mouse lympatic network graph based on anatomical data with 36 nodes and 49 edges. (b) Example simulated graph of the mouse lymphatic system. Algorithm parameters:  $N_v = 36$ ,  $N_{inp} = 13$ ,  $N_l = 5$ ,  $P_e = 0.851$ ,  $P_o = 0.66$ .

area to the nearest LN and the time for immune cells to find the antigen inside the LN. Banerjee and Moses [3] use an ODE model to estimate that, empirically, immune response times are independent of host body size.

## 3 Methods

## 3.1 Lymphatic Network Simulation Algorithm

Savinkov et al [20] developed an algorithm that generates a random directed human lymphatic network graph with no cycle from a reference human graph. We extend their work by adding another step to the algorithm to simulate T cells traveling through the circulatory system to enter LNs. The steps are given in Algorithm 1.We used data from [9] to create a reference graph of mice to compare with the simulated graph. Out of 5 input parameters in the algorithm, three parameters, number of nodes  $N_v$ , number of input nodes  $N_{inp}$ , and number of layers  $N_l$  are explicitly set to match the anatomy-based graph's properties. Based on the comparison metrics characterizing the topology of an anatomy-based graph (described in Section 3.2), the value of the other two parameters, probability of new edge creation  $P_e$  at each step and probability that the created edge connects nodes from different layers  $P_o$ , are set to produce graphs with similar topological structures.

# 3.2 Comparing simulated graphs to observation

We have used the following topological properties defined in [20] to compare the observed graph with the current state of the simulated graph for humans and mice: The number of input nodes  $N_{inp}$ , Maximum degree of graph  $\Delta G$ , Girth of the graph, g, The diameter of the graph, D, Radius of the graph, r, Average path length,  $I_G$ , The energy of the graph,  $E_n$ , The spectral radius of the graph,  $\rho$ , Edge density of the graph,  $\rho_d$ , The clustering coefficient, C (transitivity). We also introduced the following graph properties to the list: Number of separators,  $n_{sep}$ : is the number of nodes removal of which disconnects the graph  $n_{deg_i}$ : is

the number of nodes with degree i.  $G_l$ : is the average degree of nodes in each layer l and,  $n_l$ : is the number of nodes in each layer l.

Since number of node connections and layers are larger in larger animals,  $n_{deg_i}$  and  $n_l$  are also larger. Thus, the objective function has more parameters in larger animals. To produce a similar graph that matches these topological properties, we tune the parameters  $P_e$  and  $P_o$ . We collect these parameter values for the minimum value of the objective function,  $\omega$ . For a number of properties, the objective function is defined as:

$$\omega = \sum_{i=1}^{a} \left( \frac{s_i(G) - s_i(G^*)}{s_i(G^*)} \right)^2 \tag{1}$$

where

where 
$$s(G) = (n, m, n_{inp}, \Delta G, g, D, r, I_G, E_n, \rho, \rho_d, C, n_{sep}, n_{deg_1}, ..., n_{deg_{max}}, G_1, ..., G_l, n_1, ..., n_l)^T$$

This objective function penalizes the topological discrepancies of graph G from the target graph G\* and weighs them with  $(s_i(G*))^{-2}$  to bring discrepancies of different components of vector s to a single scale.

#### 3.3 Search Algorithm

To run the search algorithm, we randomly choose a source node  $n_s$  from which the T cell initiate a random walk through the graph. We consider that the LNs that contain matching DC, designated  $V' \in V$ , are distributed within the lymphatic network in three ways for different kinds of infections.

- Random Systemic: Systemic infections can spread to multiple lymph nodes throughout the body, i.e., in HIV. For this case, we assume that the V' are distributed randomly over the lymphatic network.
- Clustered: A cluster of LN can contain antigen if an animal gets a vaccine injection with inoculation dose adjusted to size, or if an animal breathes in a respiratory virus where the amount of inhaled virus is proportional to lung size. For such cases, we distribute the V' nodes in clusters. We randomly pick one node and run Breadth-First Search (BFS) to make the clusters. We exclude the circulation node 0 from being in the cluster.
- Single: If an animal steps on a thorn and gets a local infection of a fixed size, or a mosquito bite transmits an illness into the blood, then the same small amount of infection is injected into the animal regardless of its size. For both of these cases, we randomly pick one node |V'| = 1 that contain cognate DC.

We compute the time it takes for each T cell using a random walk to reach the first LNs that contains DCs holding cognate antigen. We follow Perelson and Weigel's prediction that the number of LNs in mammals scale with  $\propto M^{\frac{1}{2}}$  [18], for the random systemic and clustered scenarios,  $|V'| \propto M^{\frac{1}{2}}$ . For the uniform random and clustered V', we assume the number of LNs that are bearing the cognate antigen-bearing DCs (|V'| are 5 and 275 in mice and humans, respectively representing 7% and 3.6% of LN.

**Table 1.** Summary statistics for observed and simulated graphs of mice and humans characterizing their topological properties. For the predicted graphs, we present the statistics obtained over 10,000 graphs for human and 500 for mice.

Parameter	Mice observed graph	Mice simulated graph	Human observed graph	Human simulated graph
$\overline{G(n,m)}$	(36, 53)	(36, 49)	(996, 1117)	(996, 1029)
$N_{inp}$	13	13	357	357
Maximum degree, $\Delta G$	24	26	8	16
Girth, g	3	3	3	4
Diameter, D	4	4	40	39.96
Radius, r	3	3	30	28
Average path length, $l_G$	1.34	1.42	12.79	15.3
Energy, $E_n$	37.17	36.40	1224.5	1190
Spectral radius, $\rho$	5.81	5.91	3.51	4.18
Edge density, $\rho_d$	0.04	0.04	0.001127	0.001038
Clustering coefficient, $C$	0.12	0.11	0.027	0.0004
Number of separators, $n_{sep}$	, 5	9	401	496

# 4 Results

## 4.1 Modeled Lymphatic Network

We run the extended algorithm to generate lymphatic networks for humans and mice. Figure 1, and Figure 2 show the resulting observed and simulated graphs for mice. The first three parameters of the algorithm for mice are collected from [9]. For  $P_0$  and  $P_e$ , we take their values that give the objective function's minimum value in Equation (1). They are compared numerically in Table 1 based on the topological properties, described in Section 3.2.

From Table 1 we can see that the properties are very similar for observed and simulated graphs for mice and humans. Some properties vary slightly, but the statistic from the objective function gives the overall best match of the simulated graph to the observed graph. We collect the time data the DC takes in humans and mice respectively to reach the LN containing cognate T cell from the infected area after running the random walk, shown in Figure 4. The time for T cells to encounter a target LN is shorter in humans than in mice for random and clustered target LNs. That is because there are more target LN in humans, and we consider only the time to find the first target LN. The search to find a single V', takes much longer in humans because there are many more LN in humans (996) compared to mice (36).

# 4.2 Predicted Time

We compare the search time of a single T cell to find a target LN to actual immune response times to determine if our model predictions are reasonable. We calculate times from hop counts and estimates of the time between hops, shown in Table 2. Since we only model a portion of the overall adaptive immune response, that is, the time taken for a single T cell to conduct a random walk through the lymphatic network to find an infection, we cannot predict the speed of the overall immune response. For mice LN mean residence time in LN per hop is approximately 13 h [23], and for sheep 19 h [14]. Since sheep and humans



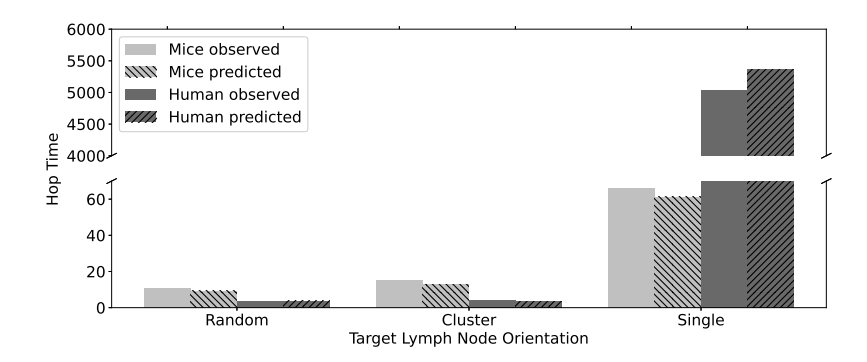


Fig. 4. Average Number of Hops to Find a LN with Cognate Antigen after running the random walk on 500 observed and algorithm-based graph of mice and human. The **random bars** represent that |V'| are randomly distributed over the graphs. There are 275 LNs containing the cognate T cell out of 996 LNs in human and 5 LNs out of 36 LNs in mice. The **cluster bars** represent |V'| are distributed in clusters over the graphs. There are 275 LNs containing the cognate T cell out of 996 LNs in human and 5 LNs out of 36 LNs in mice. The **single bars** represent that there is only one LN (|V'| = 1) chosen at random carrying the cognate T cell out of 996 LNs in human and 36 LNs in mice.

masses are similar (40 kg-160 kg for sheep [5] and 43 kg-140 kg for humans) [25], we approximate residence times in humans with those of sheep. Multiplying these residence times by the hop counts from Figure 4 results in Table 2. We find that the predicted time for a single T cell to find a LN with cognate antigen is on the same order as observed immune response times for systemic infections in mice and humans. According to [17, 15, 10, 22, 7] the mean adaptive immune response time in mice for influenza and LCMV infection is 5.3 days and in humans for SARS-CoV2 its 5.1 days [13, 8, 12]. This means that for systemic or whole-organ infections (where the number of LN increases with body mass), typical T cells can find the a LN with antigen during the time available to proliferate and amplify the growing immune response. In contrast, the time to find a single LN with antigen is orders of magnitude longer. This suggests that not many T cells would reach the single LN during the time of adaptive immune amplification. However, in small infections, a global response is likely not to be needed. We expect the T cells that reside in the local LN to be sufficient to respond to small local infection [3]. The actual timing depends on many factors, including the fraction of LN containing target DCs, V' and the number of cognate T cells searching for those DCs. We do not consider lymph vessel or blood residency times in these estimates, because those times are small relative to the time within LN [23].

**Table 2.** Predicted times for T cell to enter LN containing cognate DC based on hop count. *H. sapiens* and *M. musculus* LN residence times are taken to be 19 h. Time given in days (d).

	M. musculus			H. sapiens				
	Observed		Simulated		Observed		Simulated	
	Random	Clustered	Random	Clustered	Random	Clustered	Random	Clustered
Hops	11	15	9.3	13	3.8	4.1	3.9	3.4
Time	$5.9\mathrm{d}$	$8.3\mathrm{d}$	$5\mathrm{d}$	$7\mathrm{d}$	$3\mathrm{d}$	$3.3\mathrm{d}$	$3\mathrm{d}$	$2.7\mathrm{d}$

## 5 Discussion

We simulated the lymphatic network for mice, ran a random walk process on the resulting graph, and predicted the time for a typical T cell, searching that graph for a LN with cognate antigen. We examined three scenarios corresponding to different infection patterns: random systemic infection, clustered infection, and infection in a single LN. Our results show that the time for each T cell to search for clustered and randomly distributed systemic infections in lymph nodes are on the same order as observed immune response times to systemic infections such as influenza and COVID-19 in humans and mice. In contrast, the time for a T cell to find a single LN is far longer, requiring thousands of network hops that would take years of search time in humans or a month in a mouse. However, we suggest that such long search times for small localized infections may be adaptive. For systemic infections that require a large response, T cells quickly discover LN with DCs presenting antigen, but T cells are not recruited to small local infections when they are not needed – local infections are responded to only by the small number of T cells that already reside in the lymph node where the infection is presented on DC.

This analysis shows that the physical structure of the lymphatic network facilitates scale invariant immune response. For large and systemic infections that require a large and fast response, T cells navigate the lymphatic network to find infected LN equally fast in large and small animals. In one sense, the adaptive immune system exemplifies the kind of decentralized control typical in swarm intelligence: immune response is fast and adaptable based on the independent action of billions of immune cells that communicate locally and navigate complex tissue environments. However, the decentralized search is constrained by the network structure of the lymphatic system that provides a form of global guidance in physical space. That structure contributes to the extraordinary scalability of response.

**Acknowledgements** We thank the UNM Center for Advanced Research Computing, supported in part by the NSF, for high performance computing resources, and NSF awards 2030037 & 2020247 for funding.

#### References

- 1. Human lymphatic system 3d model. https://www.plasticboy.co.uk/store/Human\_Lymphatic\_System\_no\_textures.html (Last accessed 30 April, 2022)
- 2. Banavar, J.R., Moses, M.E., Brown, J.H., Damuth, J., Rinaldo, A., Sibly, R.M., Maritan, A.: A general basis for quarter-power scaling in animals. Proceedings of the National Academy of Sciences 107(36), 15816–15820 (2010)
- 3. Banerjee, S., Moses, M.: Scale invariance of immune system response rates and times: perspectives on immune system architecture and implications for artificial immune systems. Swarm Intelligence 4(4), 301–318 (2010)
- 4. Banerjee, S., Perelson, A.S., Moses, M.: Modelling the effects of phylogeny and body size on within-host pathogen replication and immune response. Journal of The Royal Society Interface **14**(136), 20170479 (2017)
- 5. Burrill, M.J.: Sheep. In: World Book. World Book Inc (2004)
- Cable, J.M., Enquist, B.J., Moses, M.E.: The allometry of host-pathogen interactions. PLoS One 2(11), e1130 (2007)
- De Boer, R.J., Homann, D., Perelson, A.S.: Different dynamics of cd4+ and cd8+ t cell responses during and after acute lymphocytic choriomeningitis virus infection. The Journal of Immunology 171(8), 3928–3935 (2003)
- 8. Iyer, A.S., Jones, F.K., Nodoushani, A., Kelly, M., Becker, M., Slater, D., Mills, R., Teng, E., Kamruzzaman, M., Garcia-Beltran, W.F., et al.: Dynamics and significance of the antibody response to sars-cov-2 infection. MedRxiv (2020)
- 9. Kawashima, Y., Sugimura, M., Hwang, Y.C., Kudo, N.: The lymph system in mice. Japanese Journal of Veterinary Research **12**(4), 69–78 (1964)
- Keating, R., Morris, M.Y., Yue, W., Reynolds, C.E., Harris, T.L., Brown, S.A., Doherty, P.C., Thomas, P.G., McGargill, M.A.: Potential killers exposed: tracking endogenous influenza-specific cd8+ t cells. Immunology and cell biology 96(10), 1104–1119 (2018)
- 11. Kleiber, M.: Body size and metabolic rate. Physiological reviews **27**(4), 511–541 (1947)
- 12. Koblischke, M., Traugott, M.T., Medits, I., Spitzer, F.S., Zoufaly, A., Weseslindtner, L., Simonitsch, C., Seitz, T., Hoepler, W., Puchhammer-Stöckl, E., et al.: Dynamics of cd4 t cell and antibody responses in covid-19 patients with different disease severity. Frontiers in medicine **7** (2020)
- Lei, Q., Li, Y., Hou, H.y., Wang, F., Ouyang, Z.q., Zhang, Y., Lai, D.y., Banga Nd-zouboukou, J.L., Xu, Z.w., Zhang, B., et al.: Antibody dynamics to sars-cov-2 in asymptomatic covid-19 infections. Allergy (2020)
- 14. McDaniel, M.M., Ganusov, V.V.: Estimating residence times of lymphocytes in ovine lymph nodes. Frontiers in immunology p. 1492 (2019)
- 15. Miao, H., Hollenbaugh, J.A., Zand, M.S., Holden-Wiltse, J., Mosmann, T.R., Perelson, A.S., Wu, H., Topham, D.J.: Quantifying the early immune response and adaptive immune response kinetics in mice infected with influenza a virus. Journal of virology 84(13), 6687–6698 (2010)
- Moses, M.E., Cannon, J.L., Gordon, D.M., Forrest, S.: Distributed adaptive search in t cells: lessons from ants. Frontiers in immunology 10, 1357 (2019)
- 17. Owens, S.L., Osebold, J., Zee, Y.: Dynamics of b-lymphocytes in the lungs of mice exposed to aerosolized influenza virus. Infection and immunity **33**(1), 231–238 (1981)
- 18. Perelson, A.S., Wiegel, F.W.: Scaling aspects of lymphocyte trafficking. Journal of theoretical biology **257**(1), 9–16 (2009)

- 19. Reddy, N.P., Krouskop, T.A., Newell Jr, P.H.: A computer model of the lymphatic system. Computers in biology and medicine **7**(3), 181–197 (1977)
- Savinkov, R., Grebennikov, D., Puchkova, D., Chereshnev, V., Sazonov, I., Bocharov, G.: Graph theory for modeling and analysis of the human lymphatic system. Mathematics 8(12), 2236 (2020)
- 21. Solé, R., Moses, M., Forrest, S.: Liquid brains, solid brains (2019)
- 22. Tamura, S.i., Kurata, T.: Defense mechanisms against influenza virus infection in the respiratory tract mucosa. Jpn J Infect Dis **57**(6), 236–47 (2004)
- Textor, J., Henrickson, S.E., Mandl, J.N., Von Andrian, U.H., Westermann, J., De Boer, R.J., Beltman, J.B.: Random migration and signal integration promote rapid and robust t cell recruitment. PLoS computational biology 10(8), e1003752 (2014)
- 24. Tretyakova, R., Savinkov, R., Lobov, G., Bocharov, G.: Developing computational geometry and network graph models of human lymphatic system. Computation **6**(1), 1 (2017)
- Walpole, S.C., Prieto-Merino, D., Edwards, P., Cleland, J., Stevens, G., Roberts,
   I.: The weight of nations: an estimation of adult human biomass. BMC public health 12(1), 1–6 (2012)
- 26. West, G.B., Brown, J.H., Enquist, B.J.: A general model for the origin of allometric scaling laws in biology. Science **276**(5309), 122–126 (1997)
- Wiegel, F.W., Perelson, A.S.: Some scaling principles for the immune system. Immunology and cell biology 82(2), 127–131 (2004)